

## Synthesis Method of Hemp-Derived Graphene

M. Z. Hossain\*, S. Sutradhar, M. R. Karim

Department of Chemical Engineering and Polymer Science, Shahjalal University of Science and Technology, Sylhet, Bangladesh

Received 17 September 2021, accepted in final revised form 19 January 2022

### Abstract

Graphene has attracted great attention to researchers nowadays for its electronic, optical, and mechanical properties. A key requirement for applications is the development of industrial-scale, reliable, and inexpensive production processes. In this work, we present a scalable approach of graphene synthesis from a biomass source such as hemp bast fiber which is called hemp bast fiber derived graphene (HGr). The structure and morphology of HGr are confirmed by performing several characterization techniques such as XRD, Raman spectroscopy, and TEM analysis. Mesoporosity of the HGr is confirmed by BET surface area and BJH pore size distribution analysis.

**Keywords:** Hemp bast fiber; Biochar; Hemp-derived graphene; Mesoporosity.

© 2022 JSR Publications. ISSN: 2070-0237 (Print); 2070-0245 (Online). All rights reserved.  
doi: <http://dx.doi.org/10.3329/jsr.v14i2.55694> J. Sci. Res. **14** (2), 601-606 (2022)

### 1. Introduction

Graphene is a two-dimensional single atom thick structure of  $sp^2$ -bonded carbon atoms packed in a honeycomb crystal lattice. Graphene has attracted great attention and has become one of the most widely investigated materials because of its remarkable electronic, mechanical, and thermal properties [1]. Most recently, graphene has been extensively used in energy-storage applications due to its high electrical conductivity ( $10^5$ - $10^6$  S/m), great mechanical strength (tensile strength of 130 GPa), and large specific surface area ( $\sim 2600$  m<sup>2</sup>/g) [2]. A straightforward approach to preparing graphene or graphene-like materials with their desirable properties is still a great challenge to achieve so far. In a typical chemical method, graphene is obtained from oxidation of graphite powder by modified Hummers method followed by chemical or thermal reduction. Many methods have been developed, such as chemical vapor deposition (CVD) on metal substrates [3], epitaxial growth on SiC or metal substrates [4], unzipping CNTs [5], and mechanical cleavage of graphite [1]. Most recently, preparing graphene from a renewable source is an attractive alternative to the conventional method. Wang *et al.* [6] prepared large surface area graphene-like materials such as interconnected carbon nanosheets (10-30 nm in thickness) by carbonizing hemp bast fiber using diluted sulfuric acid at 180°C

---

\* Corresponding author: [zakir-cep@sust.edu](mailto:zakir-cep@sust.edu)

followed by KOH activation in the temperature range from 700 to 800 °C in an inert gas atmosphere. In this study, we propose a synthesis method of graphene from hemp bast fiber using concentrated H<sub>2</sub>SO<sub>4</sub> and H<sub>3</sub>PO<sub>4</sub> followed by KOH activation.

## **2. Materials and Methods**

### **2.1. Materials**

Hemp bast fiber was collected from Canada. H<sub>2</sub>SO<sub>4</sub> (95-98 wt %) H<sub>3</sub>PO<sub>4</sub> (60-85 wt %), HCl (35 wt %), and KOH (85 wt %) were purchased from Merck, India. Ultra-high purity Ar (99.99 %) was purchased from Islam Oxygen Limited, Rupgonj, Narayanganj, Bangladesh.

### **2.2. Synthesis method**

Fifty mL of a mixture of concentrate H<sub>2</sub>SO<sub>4</sub> and H<sub>3</sub>PO<sub>4</sub> (6:1, v:v) along with 3 g of pre-cut hemp bast fiber were sealed in a 125 mL Teflon-lined Acid Digestion Vessel (Parr Instrument Company, Moline, Illinois, U.S.A) and kept in a preheated oven at 180 °C for 24 h. The resultant biochar was recovered by centrifuge (ca. 12000 rpm for 2 h), washed with DI water multiple times, and vacuum dried overnight at 120 °C. The dry biochar was thoroughly mixed with the desired amount of KOH using a mortar and pestle, then heated to 750 °C (0.5 °C/min) and kept at 750 °C for 1 h under argon flow in a tubular furnace. The resulting product was thoroughly washed with dilute HCl (10 wt. %) followed by DI water until the pH reached 7.0. Finally, the products were vacuum dried overnight at 120 °C.

### **2.3. Characterization**

N<sub>2</sub> adsorption and desorption isotherms data of HGr were obtained at -196 °C in a constant-volume adsorption apparatus (Tristar II 3020, Micromeritics Instrument Corporation) using 99.995 % pure N<sub>2</sub> gas (Praxair, Oakville, ON) by Brunauer-Emmett-Teller (BET) method. Porosimetry was calculated by Barrett-Joyner-Halend (BJH) methods based on the desorption branches of the isotherms. In a typical experiment, a minimum of 80 mg of sample is degassed overnight under N<sub>2</sub> flow at 150 °C, followed by adsorption-desorption analysis at -196 °C.

X-ray diffraction (XRD) measurements were performed using a Bruker D2 PHASER desktop diffractometer using Cu K $\alpha$  radiation (1.54 Å). The instrument was operated at 30 kV and 10 mA, using a scan rate of 0.2° per second in the 2 $\theta$  range from 5° to 75°. The samples are prepared as fine powders or a thin film on the sample holder.

Raman spectroscopy measurements were done using a Kaiser Optical Systems RXNI-785 with an excitation wavelength of 785 nm.

The morphology and structure of the samples were obtained from transmission electron microscopy (TEM) images (model JEOL 2010F). Before TEM analysis, the

powdered samples were dispersed in acetone by sonication and then placed and dried by normal evaporation on a copper grid covered with holey carbon film.

### 3. Results and Discussion

Table 1 shows the pore properties of HGr. KOH plays a significant role in improving the surface area and pore properties of HGr.

Table 1. Pore properties of hemp-derived graphene.

Sample	Biochar synthesis temp. (°C)	Activating reagent	Biochar :KOH ratio	BET surface area (m <sup>2</sup> /g)	Langmuir surface area (m <sup>2</sup> /g)	Pore volume (cm <sup>3</sup> /g)	Average pore size (Å)
HGr	180	KOH	1:1	1125	1494	0.64	22.9
			1:2	1410	1866	0.73	20.9

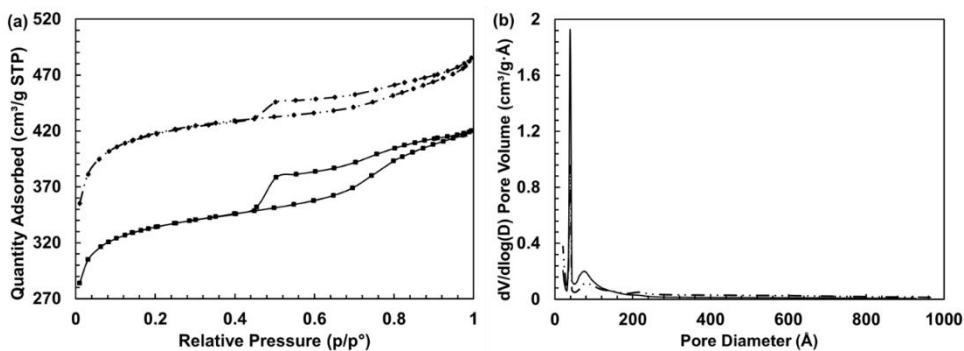


Fig. 1. (a) Nitrogen adsorption-desorption isotherm of hemp-derived graphene, (b) BJH Pore size distribution of HGr (solid and dash-dot line represents biochar: KOH = 1:1 and 1:2, respectively).

The specific surface areas and the pore size distribution plots of HGr were obtained using the BET method via N<sub>2</sub> adsorption-desorption isotherms and the BJH method, respectively. The isotherm shape in Fig.1(a) is categorized as a type IV adsorption-desorption shape with an H<sub>2</sub> hysteresis loop, at high relative pressure ranges from 0.4 to 1.0, indicating the abundance of mesopores in the structure [7]. The isotherms show two major capillary condensation steps representing the two types of mesopores present inside the samples [8]. The BJH pore size distribution reveals bi-porous mesostructure of HGr with pore sizes of 4 and 8 nm, respectively, calculated through the desorption isotherm, as shown in Fig. 1b.

Fig. 2 shows the XRD patterns of HGr. XRD pattern in the reported 2θ range is dominated by one major peak at 23.4° corresponding to the interlayer spacing of 3.7–3.8Å. Additionally, the broadened peak of HGr compared to graphene prepared by other methods can result from the turbostratic arrangement of HGr stacked sheets in small size

[9] and the formation of a new crystal structure completely different from the starting and intermediate materials [10].

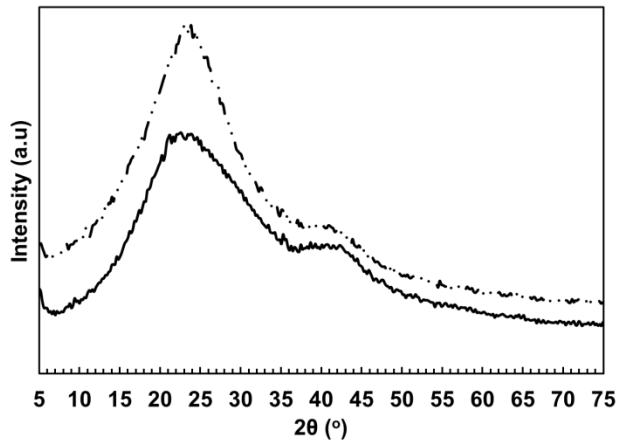


Fig. 2. XRD patterns of HGr (solid and dash-dot line represents biochar: KOH = 1:1 and 1:2, respectively).

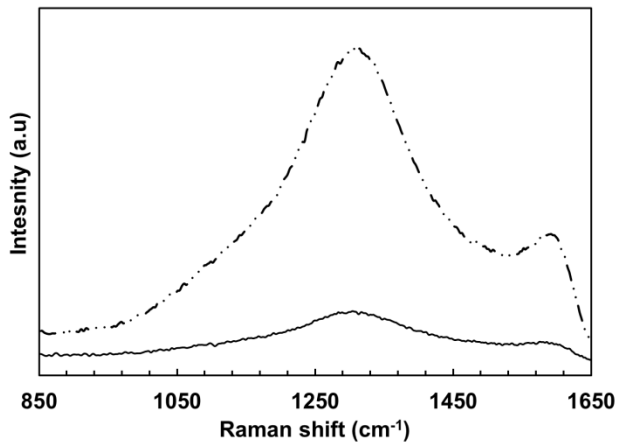


Fig. 3. Raman spectra of HGr (solid and dash-dot line represents biochar: KOH = 1:1 and 1:2, respectively).

Micro-Raman measurements are performed, meaning that individual flakes are analyzed, and data is shown in Fig. 3. Raman spectra of HGr shows both the D and G band. The G band at approximately 1593 cm<sup>-1</sup> originates from the in-plane vibration of sp<sup>2</sup> C atoms, which is ascribed to a doubly degenerate phonon mode (E<sub>2g</sub> symmetry) at the Brillouin zone center [11]. The D band peak around 1317 cm<sup>-1</sup> is a breathing mode of κ-point photons of A<sub>1g</sub> symmetry [12]. The increase of the D and G band's intensity ratio

( $I_D/I_G$ ) was due to the decrease of  $sp^2$  in-plane domain induced by the introduction of defects and disorder of the  $sp^2$  domains [13].

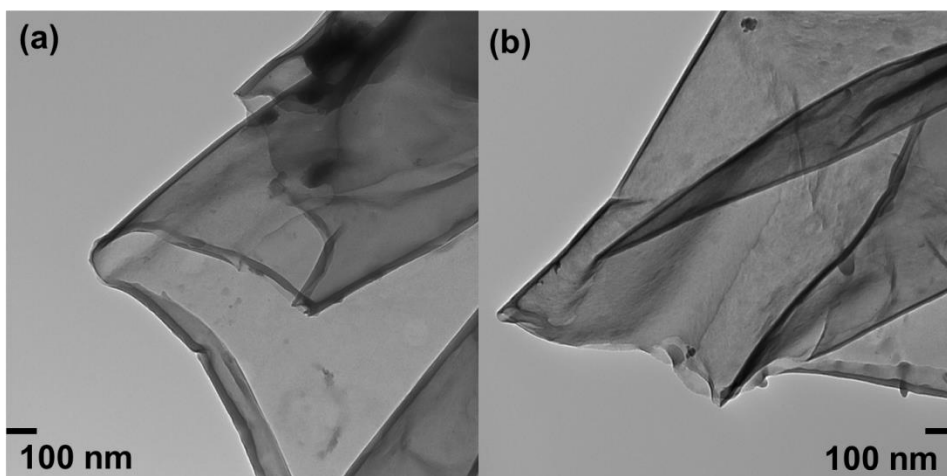


Fig. 4. TEM images of HGr (a) biochar: KOH = 1:1 and (b) biochar: KOH =1:2, respectively).

Transmission electron microscopy (TEM) is used to characterize the structure of HGr further. The TEM images (Fig. 4) indicate sheet-like morphology similar to pristine graphene. It also shows that HGr sheet tends to scroll and wrinkle, which is the intrinsic nature of graphene sheets. Dark areas indicate the thick stacking nanostructure of a few graphene layers with some oxygen functional groups. The higher transparency areas indicate much thinner films. The significantly larger surface area of the high transparency of delaminated graphene layers (of about one to few-layer thickness) is shown by HGr contrary to pristine graphene oxide sample, indicating layer delamination due to activation by KOH.

#### 4. Conclusion

Large surface area graphene was synthesized from hemp bast fiber as a sustainable resource that can be potentially used in different fields such as supercapacitors, batteries, sensors, and catalysis.

#### Acknowledgments

This work is supported by SUST (Shahjalal University of Science and Technology) Research Centre, Sylhet, Bangladesh.

**References**

1. M. Rasheed, S. Shihab, and O. W. Sabah, *J. Phy.: Conf. Ser.* **1795**, ID 012052 (2021). <https://doi.org/10.1088/1742-6596/1795/1/012052>
2. A. G. Olabi, M. A. Abdelkareem, T. Wilberforce, and E. T. Sayed, *Renew. Sustainable Energy Rev.* **135**, ID 110026 (2021). <https://doi.org/10.1016/j.rser.2020.110026>
3. Y. Song, W. Zou, Q. Lu, L. Lin, and Z. Liu, *Small* **17**, ID 2007600 (2021). <https://doi.org/10.1002/sml.202007600>
4. Y. Yu, T. Wang, X. Chen, L. Zhang, Y. Wang, Y. Niu, and J. Yu, *Light: Sci. Applicat.* **10**, 1 (2021). <https://doi.org/10.1038/s41377-021-00560-3>
5. S. Wang, Z. Huang, W. Shi, D. Lee, Q. Wang, W. Shang, and Y. Stein, *ACS Appl. Mater. Interfaces* **13-14**, 28583 (2021). <https://doi.org/10.1021/acsmi.1c01382>
6. H. Wang, Z. Xu, A. Kohandehghan, Z. Li, K. Cui, X. Tan, T. J. Stephenson, C. K. King'ondo, C. M. B. Holt, B. C. Olsen, J. K. Tak, D. Harfield, A. O. Anyia, and D. Mitlin, *ACS Nano* **6-7**, 5131 (2013). <https://doi.org/10.1021/nn400731g>
7. N. C. Joshi and S. Negi, *Inorg. Nano-Metal Chem.* **3**, 52 (2021). <https://doi.org/10.1080/24701556.2021.1980026>
8. S. Shamailla, A. K. L. Sajjad, F. Chen, and J. Zhang, *Catal. Today* **175**, 568 (2011). <https://doi.org/10.1016/j.cattod.2011.03.041>
9. S. Dubin, S. Gilje, K. Wang, V.C. Tung, K. Cha, A.S. Hall, J. Farrar, R. Varshneya, Y. Yang, and R. B. Kaner, *ACS Nano* **4**, 3845 (2010). <https://doi.org/10.1021/nn100511a>
10. T. Zhou, F. Chen, K. Liu, H. Deng, Q. Zhang, J. Feng, and Q. Fu, *Nanotechnol.* **22**, ID 045704 (2011). <https://doi.org/10.1088/0957-4484/22/4/045704>
11. Z. Ni, Y. Wang and T. Yu, Z. Shen, *Nano Res.* **1**, 273 (2008). <https://doi.org/10.1007/s12274-008-8036-1>
12. A. C. Ferrari and J. Robertson, *Phy. Rev. B* **61**, ID 14095 (2000). <https://doi.org/10.1103/PhysRevB.61.14095>
13. S. Stankovich, D. A. Dikin, R. D. Piner, K. A. Kohlhaas, A. Kleinhammes, Y. Jia, Y. Wu, S. T. Nguyen, and R. S. Ruoff, *Carbon* **45**, 1558 (2007). <https://doi.org/10.1016/j.carbon.2007.02.034>